

THE STUDY OF WATER LEAKAGE THROUGH FRACTURE IN REINFORCED CONCRETE

A. Shimmura
Obayashi Corporation, Japan;
V. E. Saouma
Department of Civil Engineering, University of Colorado, USA

Abstract

Concrete vessels are being used to store and isolate hazardous materials. However, cracks in concrete cause leakage of these hazardous materials. The objective of this study is to develop a suitable model to simulate water leakage through cracks using experimental and numerical techniques. In the experimental studies, wedge-splitting tests are performed on reinforced concrete specimens which are pressurized by water during different stages of crack propagation.

The experiments are then numerically simulated using finite element program based on the discrete crack model to analyze the behavior of cracks in concrete and interface of reinforcement. Wedge-splitting specimen of plane concrete and simple bonding test of rebar are also simulated to evaluate the crack property in concrete and interface property on reinforcement in advance. Two kinds of fluid models for two different stages of water leakage are proposed.

Key words: Reinforced concrete, Water leakage, Wedge-splitting test, Discrete crack model

1 Introduction

Concrete vessels are being increasingly used to store and isolate hazardous materials such as chemicals, liquid gas, and low level radioactive liquid

wastes. Whereas concrete itself is a relatively impermeable material, its cracks are comparatively very permeable.

Leakage through concrete of liquid and gas has been experimentally investigated in reinforced concrete by Suzuki(1992) and Iriya(1992), and the effects of water pressure on crack propagation have been experimentally studied by Brühwiler(1995). Furthermore, Reich(1993) has conducted the numerical simulation of water pressure-fracture interaction.

This paper will report a study of fracture properties and leakage flow in reinforced concrete. In the experimental studies, wedge-splitting tests were performed on reinforced concrete specimens. These specimens were loaded, and their notches were pressurized by water during different stages of crack propagation. Those experiments were then numerically simulated by finite element program of the discrete crack model. Based on the experimental and numerical investigations, simple fluid models will be proposed.

2 Experimental Tests

2.1 Test Procedure

Wedge-splitting specimens in which both inlet and outlet pipes were embedded were used as illustrated in Figure 1. Five small holes (ϕ 0.16 mm) were used to measure the inner water pressure along the propagating crack with pressure transducers. A membrane was epoxied on the surface of the specimen to prevent side water leakage.

Nine tests were conducted as shown in Table 1. The concrete mix design was governed by requirements for watertight structure and it is given in Table 2.

The experimental set-up consists of three main components: 1) mechanical wedge-splitting device; 2) hydraulic loading device; and 3) series of pressure transducers to measure the hydrostatic pressure along the fracture ligament. The mechanical load was controlled by the crack mouth opening displacement (CMOD), and a pressurized water tank provided the hydrostatic load. Water leaked through the outlet pipe was collected and its volume is measured. Specimens were loaded at a CMOD rate of 0.002 mm/sec without water pressure and they were pressurized at each 0.1 mm increment of CMOD prior to leakage (and 0.2 mm subsequently).

2.2 Test Results

Figure 2 illustrates the splitting load-CMOD curves of specimens 1, 2, and 4. The splitting load-CMOD curve of specimen 1 exhibits the typical softening behavior, however the other specimens have a drastically different response due to the reinforcement.

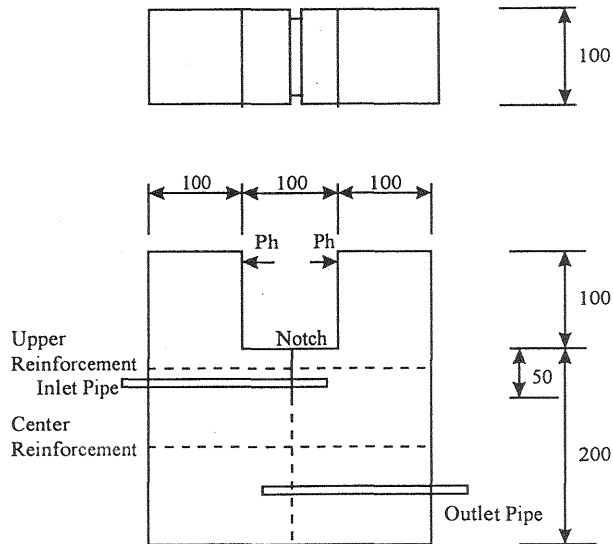


Figure 1 Dimensions of specimen

Table 1. Test matrix

Specimen Number	Inner Pressure (MPa)	Reinforcements	Arrangement of Reinforcement	Reinforcement Ratio
1	0	None		0%
2	0	ϕ 13 mm rebar	Center	0.8%
3	0	ϕ 9 mm rebar	Center	0.35%
4	0.3	ϕ 13 mm rebar	Center	0.8%
5	0.3	ϕ 9 mm rebar	Center	0.35%
6	0.3	ϕ 6 mm straight bar	Center	0.15%
7	0.3	ϕ 9 mm rebar	Upper side	0.35%
8	0.2	ϕ 9 mm rebar	Center	0.35%

Table 2. Concrete mix design (kg/m^3)

W/C ratio	Max. agg. size	Cement	Water	Sand	Aggregate 2.25 -12.5 mm	Aggregate 12.5 -25 mm	Admixture
40%	25 mm	505	202	530	503	440	$\text{C} \times 0.1\%$

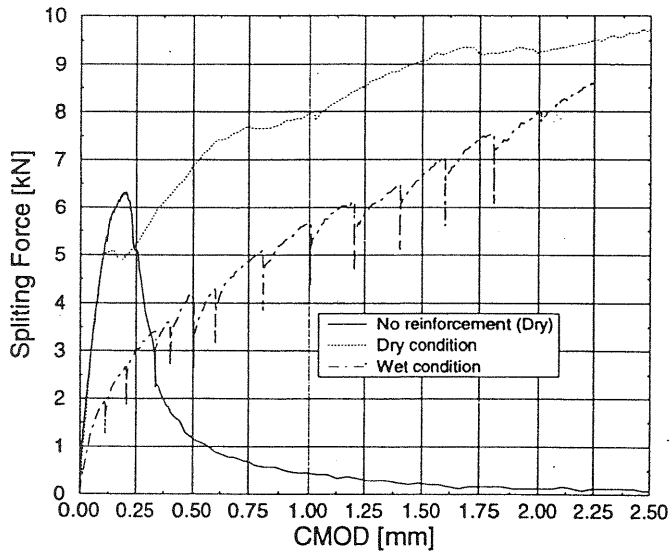


Figure 2 Load-CMOD curves of wedge splitting specimens 1, 2 and 4

Figure 3 shows that the leaking flow starts when minimum crack width which derived from the later numerical analysis becomes approximately 0.05 to 0.07 mm. Leaking rate is significantly reduced when rebars are located in the center, and it is proportional to the applied pressure.

Figure 4 shows the water pressure distribution measured by pressure transducers for specimens 6 and 7. This figure shows that the pressure is gradually built-up as the CMOD increases; however, once flow starts, the hydrostatic pressure distribution remains constant. During water flows, the pressure above the reinforcement is about the same as the pressure applied through the inlet pipe, but below the reinforcement, there is a linear pressure decrease from full pressure to zero at the outlet.

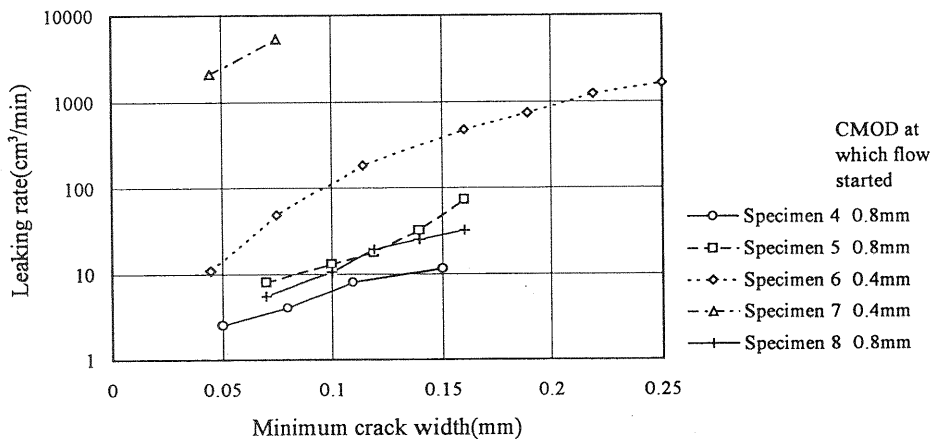


Figure 3 Flow rate and minimum crack width relations

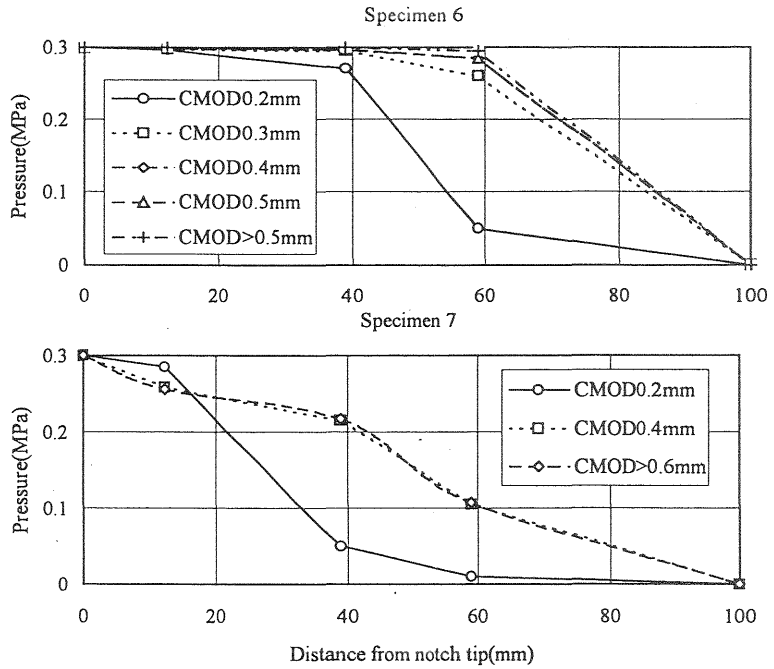


Figure 4 Pressure distribution of specimen 6 and 7

3 Finite Element Simulation

3.1 Analysis Procedures

The objective of these analyses is to identify the interface properties of a crack and bond properties of the steel in the presence of an internal hydrostatic pressure. Another objective of this simulation is to capture the crack width along the crack from which fluid models could be developed.

Analyses were performed with the non-linear finite element method which uses an interface crack model. This model uses the failure function with the following failure surface

$$F = \tau^2 - 2c \tan \phi_f (\sigma_t - \sigma) - \tan^2 \phi_f (\sigma_t - \sigma)^2 = 0 \quad (1)$$

where c is the cohesion, ϕ_f the friction angle, σ_t the interface tensile strength, τ the tangential component of interface traction, and σ the normal interface traction. c and σ_t are themselves functions of the norm of inelastic displacement u_{ieff} . The adopted softening laws are illustrated in Figure 5.

G_I and G_{II} are fracture energy of mode I and mode II respectively. The break point coordinates can be expressed by Wittman(1988) as:

$$s_l = 0.25 \sigma_{l0} \quad (2)$$

$$w_l = 0.75G_F / \sigma_{t0} \quad (3)$$

$$w_c = 5G_F / \sigma_{t0} \quad (4)$$

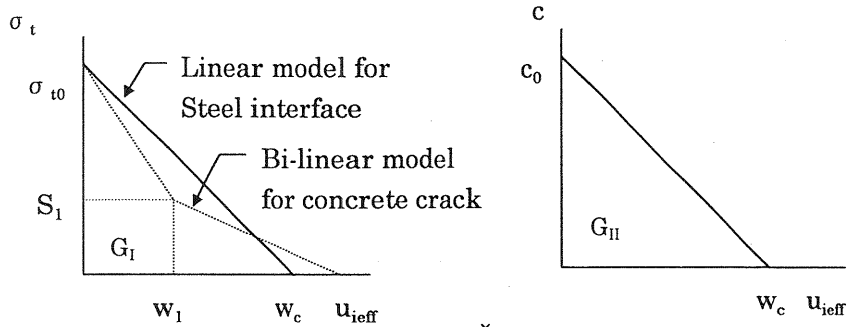


Figure 5 Softening law (Červenka 1994)

3.2 Simulation of experiments in dry condition

The load-CMOD relation of a wedge-splitting specimen of plain concrete is first simulated to identify the tensile strength and fracture energy G_I . The optimized model properties are shown in Table 3.

Table 3 Summary of constitutive properties

	Crack	Steel Interface
Width	Thickness of concrete	Circumference of reinforcement. Half circumference for large confinement in one direction.
Normal stiffness	5640N/mm ³	2820 N/mm ³
Tangential stiffness	2360 N/mm ³	1160 N/mm ³
Tensile strength	2.35 MPa	2.35 MPa
Cohesion	6 MPa	22.0 MPa for rebar 11.0 MPa for straight bar
Angle of friction	60 deg	50 deg (Dry rebar) 40 deg (Wet rebar) 30 deg (Wet straight bar) 10 deg (Wet rebar close to inner side)
Angle of dilatancy	45 deg	1.0 deg
Max. inelastic displacement of dilatancy.	0.7 mm	0.7 mm
Fracture energy G_I	0.14N/mm (Dry) 0.05N/mm (Wet)	0.14 N/mm
Fracture energy G_{II}	0.50 N/mm	55.0 N/mm

Next, in order to determine appropriate material properties to be used in interface element between steel and concrete, the pull out tests reported by Soroushian(1991) are analyzed. In these tests, ϕ 20mm rebars confined by ϕ 10mm rebars are pulled out by a hydraulic jack under sliding displacement control. The finite element model of two-dimensional plane stress elements for both the concrete and the reinforcement are used. Interface elements are inserted on both sides of rebar to properly model the bond. The model properties determined from this analysis are summarized in Table 3 and are subsequently used in other ones.

Subsequently, dry wedge-splitting specimens with rebar (specimens 2 and 3) are analyzed with two sets of interface elements, one vertically along the crack path, and another one horizontally along both sides of the reinforcement. It should be noted that the total width of the interface elements modeling the bond was reduced by one half of the circumference. The reason of this reduction is the high confining (flexural) stresses at the end of the rebars which increased the bond strength.

3.3 Simulation of experiments in wet condition

The wet specimens (specimens 4-8) are simulated to evaluate the fracture and bonding properties and crack width along the cracks under wet conditions.

Brühwiler(1995) indicated that hydrostatic pressure reduces the fracture energy of concrete and proposed the following expression of reduced fracture energy:

$$G_{Iw} = G_I (1.01 - 1.60 p_{wo} + 0.72 p_{wo}^2) \quad (5)$$

where G_{Iw} is the fracture energy reduced by water pressure, G_I is a fracture energy under the dry condition, and p_{wo} is the applied water pressure expressed in MPa.

Through a series of analyses, it was determined that the fracture energy of concrete and the friction angle of steel interface should be reduced under hydrostatic pressures as shown in Table 3. Fracture energy under wet condition is smaller than the estimated value from the above equation.

4. Fluid model in the crack

We distinguish two cases: one in which there is no flow along the crack and another in which the crack reached the outlet pipe with leakage.

4.1 Hydrostatic pressure model without flow

Reich(1993) proposed the following pair of cubic polynomials of crack width to model the transition of water pressure from zero to full applied pressure in plain concrete along the fracture process zone in case of no

flow.

$$p = p_{w_0} \left(a_1 + b_1 \left(\frac{w}{w_{w_0}} \right) + c_1 \left(\frac{w}{w_{w_0}} \right)^2 + d_1 \left(\frac{w}{w_{w_0}} \right)^3 \right) \quad (w_0 < w < w_l) \quad (6)$$

$$p = p_{w_0} \left(a_2 + b_2 \left(\frac{w}{w_{w_0}} \right) + c_2 \left(\frac{w}{w_{w_0}} \right)^2 + d_2 \left(\frac{w}{w_{w_0}} \right)^3 \right) \quad (w_l < w < w_{w_0}) \quad (7)$$

where p is the water pressure in the crack, w is the crack width, w_0 is the crack width below which water pressure is zero, w_{w_0} is the crack width above which water pressure is equal to the full applied pressure, and w_l is the crack width at a break point of the bilinear softening law. w_0 and w_{w_0} are the functions of applied pressure and tensile strength of concrete.

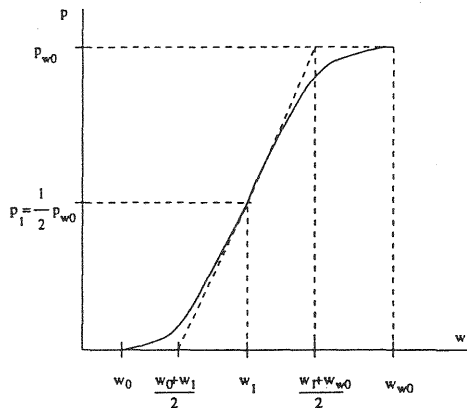


Figure 6 Reich's model of pressure transition by a pair of cubic

Table 4 summarizes w_0 and w_{w_0} identified from the experimental data, and Figure 7 shows the measured and calculated pressure distributions of specimen 5 using these w_0 and w_{w_0} values. We observe that w_0 and w_{w_0} in reinforced specimens are larger than the values recommended by Reich(1993) for plain concrete. The calculated water pressure distributions diverge from the measured pressure as CMOD increases because the crack tip reaches the outlet and the water begins to flow in the crack.

Table 4 Water pressure transition properties of Reich's model

Pressure	0.3MPa					0.2MPa	
Case	Reich's model	Specimen 4	Specimen 5	Specimen 6	Specimen 7	Reich's model	Specimen 8
$w_0(mm)$	0.008	0.008	0.018	0.018	0.018	0.006	0.020
$w_{w_0}(mm)$	0.040	0.050	0.050	0.070	0.080	0.044	0.100

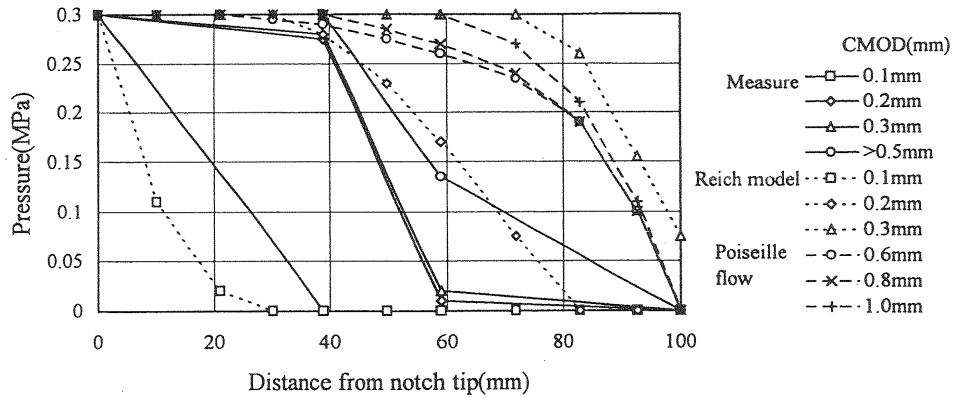


Figure 7 Simulated water pressure of specimen 5

4.2 Leaking flow model

While fluid is flowing along a concrete crack, the flow is assumed to be a two-dimensional steady flow between two parallel plates, i.e. Poiseuille flow.

The flow rate of incompressible steady flow between two parallel plates with an applied pressure gradient is

$$q = \frac{1}{12} \frac{w^3 b}{\mu} \left(-\frac{dp}{dx} \right) \quad (8)$$

where q is the flow rate, b is the breadth of flow, w is the distance between two parallel plates, μ is the coefficient of fluid viscosity, and p is the pressure.

In the case of actual concrete crack, its width is not constant; therefore, we introduce the effective crack width for Poiseuille flow.

$$w_{pf} = R_{pf} w \quad (w < w_a) \quad (9)$$

where R_{pf} is a reduction factor obtained from experimental data. Using crack width derived from the finite element simulation, we determined the R_{pf} and w_a which are tabulated in Table 5. We observe that the reduction factor decrease with increased bar size, and this reduction is not needed in the case that the reinforcement is located upper.

Table 5 Coefficients of effective crack width for Poiseuille flow model

Specimen	4	5	6	7	8
R_{pf}	0.075	0.10	0.22	1.20	0.11
w_a	0.30mm				

5 Conclusion

From this investigation, the following general conclusions can be drawn:

- Leaking flow rate is reduced if the rebar is placed close to the outlet.
- Interface elements can properly model the bond between steel and concrete. The effective bond area had to be reduced for the large confinement by compressive stress in one direction.
- Internal hydrostatic pressure reduces not only the fracture energy of concrete, but also the friction angle of reinforcement interface.
- Existing models for fluid fracture interaction, developed for unreinforced concrete, are satisfactory. However, when a flow is present, a Poiseuille flow model should be adopted.

6 References

- Brühwiler, E. and Saouma, V.E.(1995) Water fracture interaction in concrete; part i fracture properties. **ACI Material Journal**, 92(3), 296-303.
- Červenka, J.(1994) Discrete crack modeling in concrete structure. Ph. D thesis, University of Colorado, Boulder.
- Iriya, K., Itoh, Y., and Hosoda, M.(1992) Experimental study on the water permeability of reinforced concrete silo for radioactive waste repository. **Nuclear Engineering and Design**, 138, 165-170.
- Reich, R.W.(1993) On the marriage of mixed finite element methods and fracture mechanics: an application to concrete dams. Ph.D thesis, University of Colorado, Boulder.
- Soroushian, P., Choi, K., Park, G. and Aslani, F.(1991) Bond of deformed bars to concrete: effect of confinement and strength of concrete, **ACI Material Journal**, 88(3), 227-232.
- Suzuki, T., Takiguchi, K., and Hotta, H.(1992) Leakage of gas through concrete cracks. **Nuclear Engineering and Design**, 133,121-130.
- Wittman, F.H. Rokugo, K., Brühwiler, E., Mihashi, H., and Simonin, P.(1988) Fracture energy and strain softening of concrete as determined by means of compact tension specimens. **Materials and Structure**, 21,21-32.